Research Article

Magdaléna Doleželová, Lenka Scheinherrová, and Alena Vimmrová*

# Study of gypsum composites with fine solid aggregates at elevated temperatures

https://doi.org/10.1515/secm-2021-0025
received November 10, 2020; accepted January 28, 2021

**Abstract:** The structure and behaviour of two gypsum composites after exposition to elevated temperatures were investigated. The silica sand and fine basalt aggregate were used as solid fillers. The changes in structure and composition at temperatures from 50 to 1,000°C were investigated by scanning electron microscopy and X-ray diffraction together with the size and strength of the samples and their pore size distribution. The structure of gypsum matrix changed significantly at 1,000°C in both composites, while the aggregate particles were not changed. It was found that even if the silica sand is considered as less suitable filler at high temperatures because of its volume changes, the gypsum with sand performed better than gypsum with basalt at the highest temperatures, because the shrinkage of the gypsum matrix was compensated by the increase in the volume of aggregate. The final volume change at 1,000°C was 3.5% in composite with silica sand and 6.8% in composite with basalt. The residual compressive strength of both composites was about 9.4%. No cracks appeared in the samples and no spalling was observed.

**Keywords:** gypsum composite, elevated temperatures, microstructure, porosity, properties

## 1 Introduction

Calcined gypsum ($CaSO_4 \cdot 0.5H_2O$) is considered to be good fire-resistant material and it is often used as a fire protection for other, less resistant materials as a steel or wood. The high fire resistance of gypsum is caused by the chemically bonded water in the crystals. The hardened gypsum paste consists mostly of calcium sulphate dihydrate ($CaSO_4 \cdot 2H_2O$) after mixing of calcined gypsum powder with water according to equation (1) [1], and it contains about 21% by mass of bonded water.

$$CaSO_4 \cdot 0.5H_2O + 1.5H_2O \rightarrow CaSO_4 \cdot 2H_2O. \quad (1)$$

When hardened gypsum is heated, the bonded water is released gradually and until the dehydration is finished, the gypsum temperature stays under 150°C because released water vapour cools it [2]. Firstly the calcium sulphate hemihydrate (equation (2)) and then calcium sulphate anhydrite (equation (3)) are formed when gypsum paste is heated [1].

$$CaSO_4 \cdot 2H_2O \rightarrow CaSO_4 \cdot 0.5H_2O + 1.5H_2O, \quad (2)$$

$$CaSO_4 \cdot 0.5H_2O \rightarrow CaSO_4. \quad (3)$$

Anhydrite remains in the material until the temperature of the decomposition is achieved (about 1,300°C) and gypsum is decomposed into calcium oxide, sulphate dioxide, and oxygen (equation (4)). Several forms of anhydrite are formed during the heating – firstly anhydrite III (slowly soluble), then anhydrite II (insoluble), and finally anhydrite I (instable, after cooling returns to anhydrite II) [1].

$$CaSO_4 \rightarrow CaO + SO_2 + O_2. \quad (4)$$

It was found that even after heating to 1,000°C the gypsum samples maintained their integrity and they also preserved some residual strength [3,4]. The main problem is that the gypsum exhibits significant shrinkage after exposition to the high temperature [5]. The shrinkage can be reduced by utilization of fillers, e.g. vermiculite or perlite. These fillers are commonly used in the commercial products, but they significantly reduce the mechanical properties of the gypsum [6]. Common nonporous fillers are not used in the gypsum products very often, because the gypsum does not shrink at normal temperatures [7]. Nevertheless, these fillers can reduce the volume changes of gypsum at higher temperatures.

The silica sand is generally not considered suitable for these purposes, because even if it is chemically stable under 1,000°C, it exhibits significant volume changes at temperatures

* **Corresponding author: Alena Vimmrová,** Department of Material Engineering and Chemistry, Faculty of Civil Engineering, Czech Technical University in Prague, Thakurova 7, 166 29 Prague 6, Czech Republic, e-mail: vimmrova@fsv.cvut.cz
**Magdaléna Doleželová, Lenka Scheinherrová:** Department of Material Engineering and Chemistry, Faculty of Civil Engineering, Czech Technical University in Prague, Thakurova 7, 166 29 Prague 6, Czech Republic

over 500°C, caused by the phase transformation of $SiO_2$. The first increase in volume (about 1.4%) occurs at 573°C and it is caused by the inversion between α- and β-quartz forms. The second volume increase (about 14.8%) is caused by the tridymite formation at 870°C [8,9]. Nevertheless, the increase in volume can be advantageous when used in the gypsum matrix, because the sand expansion could act against the gypsum shrinkage.

The influence of two types of fine solid aggregates (silica sand and basalt) on the behaviour and structure of gypsum composites exposed to the high temperatures was studied. Composite with silica sand was used as a reference material and basalt was chosen to improve the fire behaviour of gypsum composite. The gypsum composites were heated up to 1,000°C, and their structure and properties were investigated and compared to each other.

## 2 Materials

The gypsum plaster (calcium sulphate hemihydrate) is a commercially available product (producer Saint-Gobain Construction Products CZ, branch RIGIPS, Czech Republic), prepared from flue gas desulphurization gypsum (calcium sulphate dihydrate). Silica sand (CEN standard sand according EN 196-1 [10], producer Filtrační Písky, Ltd., Czech Republic) and crushed basalt (producer KAMEN Zbraslav, Ltd., Czech Republic) were used as fine aggregates. Their granulometries obtained by the sieving test and laser particle size analysis are shown in Figures 1 and 2, respectively. Both aggregates were designed as a fraction 0–2 mm, but from the distribution curves can be seen, that basalt contained also 13% of particles larger than 2 mm. Basalt also contained rather high amount of particles under 40 μm, while silica sand had fines with the size 40–100 μm mostly. The specific gravity, bulk density, and average surface roughness of aggregates are given in Table 1. Surface roughness of all aggregates is rather high, because both were crushed; nevertheless, basalt aggregate had rougher particles than sand.

Set retarder Retardan 200 P (producer SIKA, Germany) was used in both composites.

The chemical composition of raw materials obtained by X-ray fluorescence (XRF) analysis is presented in Table 2, and their mineral composition obtained by X-ray diffraction (XRD) analysis is given in Table 3. The small amount of calcite in gypsum was caused by its origin from wet flue gas desulfurization. The standard sand contained only quartz $SiO_2$.

Results of thermal analysis of raw materials are given in Figure 3. Figure 3a shows the thermogravimetric

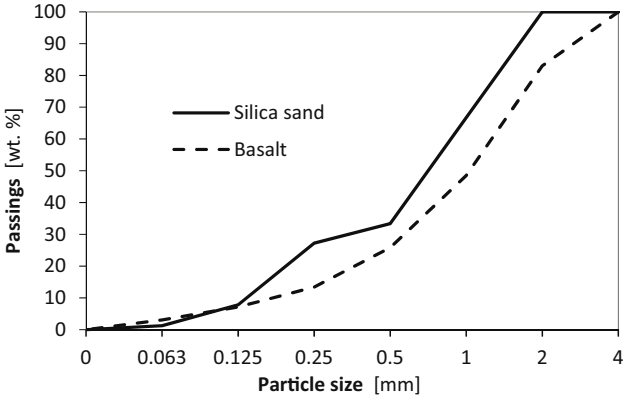


**Figure 1:** Particle size distribution of aggregates, obtained by sieving.

(TG) curves of raw materials, and Figure 3b shows the differential scanning calorimetry (DSC) curves. The biggest relative mass change of gypsum powder occurred between the temperature 100 and 200°C, which is typical for the dehydration of bassanite ($CaSO_4 \cdot 1/2H_2O$). The second mass loss between 700 and 800°C was caused by the decomposition of calcite (residue of flue gas desulfurization) and muscovite, and the endothermic peak in DSC curve of gypsum corresponds to the decomposition. There was no mass loss of silica sand, because quartz is thermally stable under 1,000°C. The endothermic peak in DSC curve of sand corresponds to the phase change of quartz. The mass loss of basalt was caused by the dehydration of hydrated minerals – muscovite, analcime, and illite [11,12].

## 3 Methods

*Chemical composition* of raw materials was determined by XRF method using device Spectroscan MAKC GVII

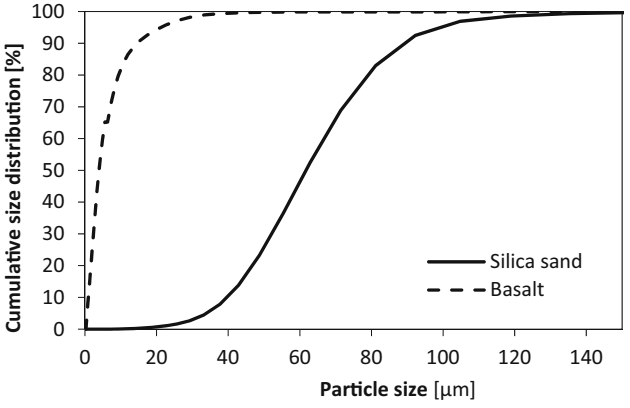


**Figure 2:** Distribution of finest particles, obtained by laser analysis.

**Table 1:** Specific gravity and bulk density of aggregates

| Aggregate | Specific gravity | Bulk density | Grain surface roughness |
|---|---|---|---|
| | (kg/m$^3$) | | (μm) |
| Silica sand | 2,831 | 2,575 | 591 |
| Basalt | 3,015 | 2,631 | 633 |

**Table 2:** Chemical composition of gypsum, silica sand and basalt

| Oxide | Gypsum | Standard sand | Basalt |
|---|---|---|---|
| | | (wt%) | |
| $Na_2O$ | | | 3.3 |
| MgO | | | 7.3 |
| $Al_2O_3$ | 0.4 | 1.1 | 17.2 |
| $SiO_2$ | 0.6 | 97.7 | 42.2 |
| $SO_3$ | 53.9 | | |
| $K_2O$ | | | 1.2 |
| CaO | 44.5 | 0.2 | 12.7 |
| $TiO_2$ | | | 3.2 |
| $Fe_2O_3$ | | 0.4 | 11.6 |
| others | 0.6 | 0.6 | 1.3 |

(Spectron Optel, Russia). *Mineral composition* was determined by XRD analysis by difractometer PANalytical Aeris (PANalytical Corporation, The Netherlands), equipped with a CoKα tube operating at 40 kV and 7.5 mA was used. Data were evaluated by Rietveld refinement using Profex software (ver. 3.12.1) [13].

*Thermal analysis* – DSC and TG were made by the Labsys Evo device (Setaram, Lyon, France). The experiment was performed in the temperature range from 25 to 1,000°C in an argon atmosphere with a flow rate 40 mL/min and heating rate 5°C/min.

*Particle size distribution* of aggregates was determined by the sieving test according EN 933-1 [14], and the size of fines was measured by laser particle size analyser Bettersizer S3 Plus (Bettersize Instruments Ltd., China).

*Microstructure* of tested materials was observed by the scanning electron microscopy (SEM) using Phenom XL electron microscope (Phenom, NL). Samples (several milligrams) were taken from the dried fractured material after strength tests. SEM samples were not coated or polished, because gypsum materials provide good images even without the coating and the polishing damages the microstructure of gypsum because of its fragility. *Surface roughness* of the aggregate particles was also determined by 3D Roughness Reconstruction software application of Phenom microscope. The software is based on "shape from shading" principle.

*Bulk density* $\rho_B$ [kg/m$^3$] of aggregates and composites was calculated from their dry mass $m$ [kg] and volume $V$ [m$^3$] according to equation 5.

$$\rho_B = \frac{m}{V}. \quad (5)$$

Volume of aggregates was found according to Czech technical standard ČSN 72 1171 [15] by the immersion of the known mass of aggregate in measured amount of water in the volumetric cylinder. Dry composite samples (prisms) were weighed, their dimensions were measured by digital calliper, and volume of sample prisms was calculated from the dimensions.

**Table 3:** Mineral composition of raw materials

| Mineral | | Gypsum | Standard sand | Basalt |
|---|---|---|---|---|
| | | | (wt%) | |
| Bassanite | $CaSO_4{\cdot}1/2H_2O$ | 88.5 | | |
| Anhydrite | $CaSO_4$ | 5.8 | | |
| Calcite | $CaCO_3$ | 3.8 | | |
| Muscovite | $KAl_2(AlSi_3O_{10})(OH)_2$ | 1 | | 8.6 |
| Quartz | $SiO_2$ | | 100.0 | |
| Diopside | $CaMgSi_2O_6$ | | | 43.8 |
| Nepheline | $(Na,K)AlSiO_4$ | | | 9.8 |
| Plagioclase | $NaAlSi_3O_8$–$CaAl_2Si_2O_8$ | | | 10.2 |
| Analcim | $NaAlSi_2O_6{\cdot}H_2O$ | | | 8.1 |
| Forsterite | $Mg_2SiO_4$ | | | 5.4 |
| Biotite | $K(Mg,Fe)_3(AlSi_3O_{10})(F,OH)_2$ | | | 2.1 |
| Illite | $K_{0.65}Al_2(Al_{0.65}Si_{3.35}O_{10})(OH)_2$ | | | 2.2 |
| Magnetite | $Fe^{2+}Fe^{3+}_2O_4$ | | | 3.6 |
| Others | | 0.9 | | 6.2 |

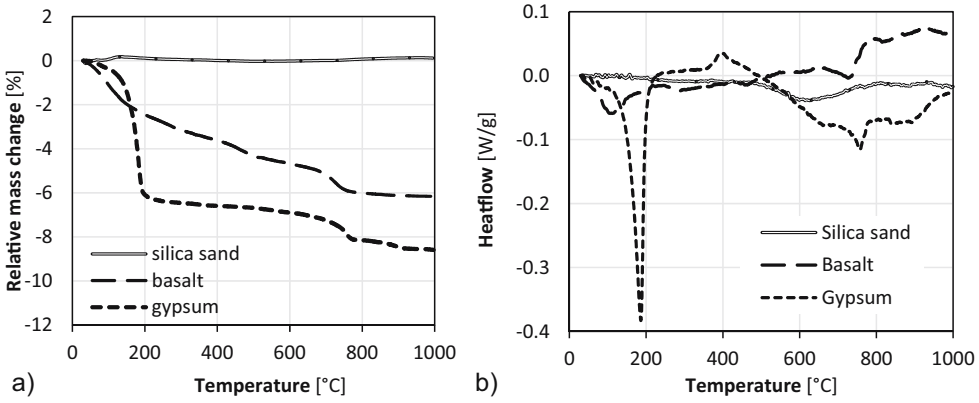


**Figure 3:** Thermal analysis of raw materials. (a) TG and (b) DSC curves.

*Specific gravity* $\rho$ [kg/m$^3$] of all the materials was determined by helium pycnometry, using the apparatus Pycnomatic ATC (Porotec, Germany).

*Volume change* of sample prisms after heating was calculated as a percentage change of volume of the sample before and after heating. The dimensions of samples were measured by the digital calliper before and after heating, and the volume was calculated from them.

*Total porosity p* [%] of composites was calculated according to equation 6 from relationship between the bulk density $\rho_B$ and specific gravity $\rho$. *Pore size distribution* was determined by mercury intrusion using device Pascal 140 + 440 (Thermo Electron, Italy).

$$p = 1 - \frac{\rho_B}{\rho} \times 100 \ [\%]. \quad (6)$$

*Bending and compressive strength* of gypsum composites after exposure to the elevated temperatures were tested according to standard EN 13454-2 [16] on the standard sample prisms (40 × 40 × 160 mm) by the mechanical testing machine FP 100 (VEB Industriewerk Ravenstein, Germany). Bending experiment was performed as a standard three-point bending test with the distance of supports 100 mm and the load in the centre between the supports. Compressive strength was measured on the halves of the specimens left over after the bending test. The prism halves were centred laterally to the auxiliary platens with the size 40 × 40 mm (Figure 4), which exactly determined the compressive area (because of irregular geometry of fractured sample).

Samples of tested materials were exposed to the *elevated temperatures* 50, 100, 200, 400, 600, 800, and 1,000°C. The temperature 50°C was used as a reference temperature, because no changes were expected yet, materials were only dried. The climatic chamber Ecocell 22 (BMT Medical Technology s.r.o., Czech republic) was used for temperatures 50–200°C and the furnace (CLASIC CZ, Ltd., Czech Republic) was used for higher temperatures. The temperature increase was 1°C/min until the required temperature was achieved. The temperature was maintained for 4 h. Scheme of heating is given in Figure 5. Then the samples were left to cool in the oven and after that in the laboratory until their temperature was equal to the room temperature (21 ± 2°C). One set of samples for each type of aggregate was exposed to each temperature.

## 4 Design and preparation of composites

The composition of tested composites was designed in such way that the volume of all solid components was the same in both materials for better comparison of their structures. The composite with standard sand had the mass ratio of gypsum binder and sand 1:3 as given in EN 13454-2, and the volume of sand was calculated from its bulk density and mass. Then the mass of basalt

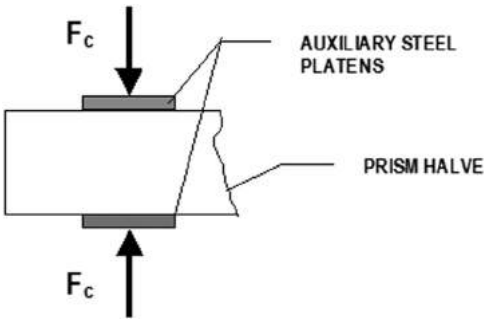


**Figure 4:** Scheme of compressive test.

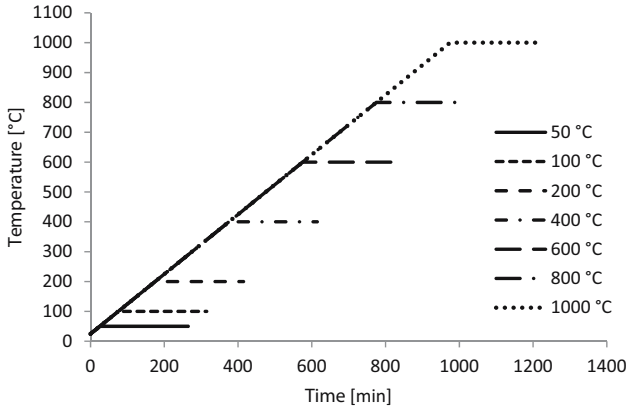


**Figure 5:** Heating scheme.

aggregate was calculated from basalt bulk density and volume of standard sand so that the volume of aggregates in the materials was the same. The amounts of gypsum and setting retarder were equal in both composites.

The amount of water was established for the same workability of both composites (flow test diameter 165 ± 5 mm). Composition of both tested materials is given in Table 4. The amount of water in composite with basalt aggregate was higher because of the higher content of very fine particles in this aggregate, as can be seen in Figure 2.

Preparation of composites was performed according to EN 196-1 [10]. Retarding agent was added to the measured amount of water in the mixing bowl and mixed together until the retarder dissolved. Dry gypsum was poured gradually into the water and bowl was put into the automatic mixing machine. Mixing included 30 s of slow mixing (140 rpm), then the aggregate was added during another 30 s of slow mixing, then 30 s of fast mixing (285 rpm). After that there was pause for 90 s to clean the bowl walls and finally the material was mixed at high speed for another 60 s.

Materials were poured into the rectangular moulds (set of three samples) immediately after mixing and compacted by 60 jolts at jolting table. The surface of samples was levelled by metal knife. The samples were removed from moulds after 3 h and stored in the laboratory (temperature 21 ± 2°C, humidity 55 ± 5%) until their exposure to the high temperatures.

Seven sets of samples were prepared from each composite; one set consisted from three standard rectangular samples with the size 40 × 40 × 160 mm. One set of each composite (GS and GB) was exposed to the particular temperature (50, 100, 200, 400, 600, 800, and 1,000°C) and after that the strength was tested and structure was evaluated.

# 5 Results and discussion

## 5.1 Thermal analysis of composites

TG and DSC curves of tested composites are given in Figure 6. There can be seen that the curves of composites corresponds with the curves of raw materials, which indicates that there was no chemical interaction between the gypsum and aggregates. The mass loss of the composite with basalt GB is higher than mass loss of the composite with sand GS, similar to the behaviour of pure aggregates (Figure 3). DSC curves of both composites are similar. Double peak between 100 and 200°C is typical for gypsum paste and it was caused by the gradual dehydration of gypsum paste ($CaSO_4 \cdot 2H_2O$) firstly to the bassanite ($CaSO_4 \cdot 1/2H_2O$) and then to the anhydrite ($CaSO_4$).

## 5.2 Microstructure of composites

The microstructure of both composites was studied after exposition to the each temperature. The changes in structure at the particular temperatures can be seen in Figure 7 for composite with silica sand GS and in Figure 8 for composite with basalt aggregates GB. There can be seen that while the aggregate particles did not change significantly, the structure of gypsum paste changed substantially. At 50°C, the gypsum crystals were thin, needle like with smooth surface. At the temperatures between 100 and 200°C the crystals started to crack and break, and the process continued to 800°C. After 800°C the structure changed dramatically – the crystals were shorter and

**Table 4:** Composition of tested materials (amount for one batch)

| Composite marking | Used aggregate | Gypsum | Aggregate | Retardan | Water |
|---|---|---|---|---|---|
| | | | (g) | | (mL) |
| GS | Silica sand | 450 | 1350.0 | 0.09 | 270 |
| GB | Basalt | 450 | 1379.4 | 0.09 | 330 |

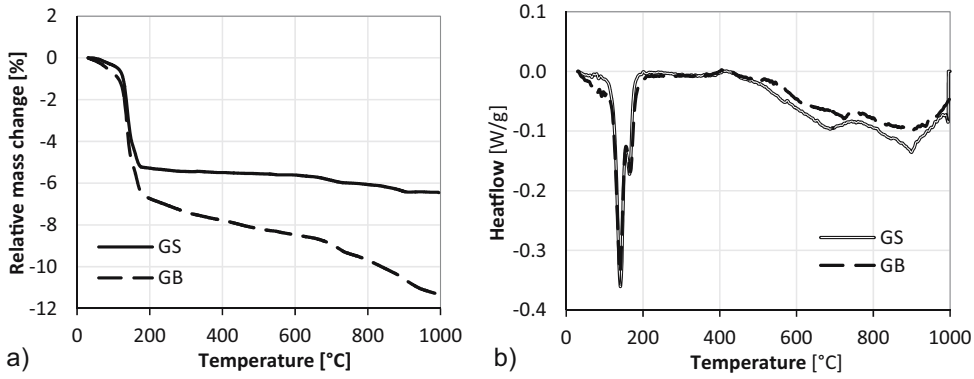


**Figure 6:** Thermal analysis of composites: (a) TG and (b) DSC.

thicker and squeezed to each other closely. The change took place in both composites, but it was more pronounced in the composite with basalt and the crystals were bigger in this composite. The process of crystals change started already before 800°C, the regions with cracked crystals with original shape and also regions with changed crystals were found (Figure 9).

It can be also seen that the contact between sand particles and gypsum paste in GS composite was disrupted at 600°C, which corresponds with the phase transformation and first volume change of silica sand. On the contrary, the transition zone between the gypsum and aggregate particle was intact even at 1,000°C.

## 5.3 Basic physical characterization of composites

The samples of both composites maintained their shape and integrity even after the exposition to the highest temperature 1,000°C, and there were no visible cracks on their surface (Figure 10), only the colour changed slightly. No spalling was observed during heating.

The basic physical characteristics of both composites at all temperatures are presented in Tables 5 and 6.

The bulk density and specific gravity of composite with basalt are higher because basalt was heavier than silica sand (Figure 11). The changes in specific gravity of GS composite were mainly caused by the changes in specific gravity of phases in gypsum matrix. The specific gravity of both materials decreased between 50 and 100°C, because the hydration of all bassanite to gypsum was not yet finished at 50°C and continued till 100°C. The decrease corresponds to the fact that specific gravity of bassanite (2.62 g/cm$^3$) is higher than specific gravity of gypsum (2.31 g/cm$^3$). After that the specific gravity increased slightly to the 400°C and then it was stable to 800°C in GB composite and to 1,000°C in GS. It corresponds to the phases changes of gypsum paste. Between 100 and 1,000°C the gypsum was dehydrated to the bassanite again and then to the anhydrite III (specific gravity 2.58 g/cm$^3$) and finally to anhydrite II (specific gravity 2.98 g/cm$^3$) [1]. The changes in density of composite with silica sand were smaller, because while the density of gypsum increased with temperature, the density of silica sand decreased (from 2.65 to 2.25 g/cm$^3$) [9].

The bulk density of both composites was similar and it did not change significantly with the temperature. The higher porosity of GB composite was caused mainly by the higher amount of water in the material.

The volume changes of both composites can be seen in Figure 12. The slight increase in volume at 100°C was caused by the hydration of residual bassanite in gypsum paste, because volume of gypsum slightly increases during hydration [2]. After that the volume of both composites decreased. The volume changes in composite with silica sand were significantly smaller, because the shrinkage of gypsum paste was compensated by the expansion of the sand. Even a slight increase in volume can be seen between 600 and 800°C, which corresponds with the second phase change of silica sand. The final shrinkage at 1,000°C was 3.5% in GS and 6.8% in GB material. Even if the shrinkage of material with basalt was nearly two times bigger than in material with silica sand, both values are significantly smaller than the shrinkage of pure gypsum paste, which could achieve even more than 50% [4].

Pore size distribution is given in Figure 13a (material GS) and Figure 13b (material GB). The distribution curves of both materials dried at 50°C had similar shape; they had mostly unimodal distribution which is typical for the gypsum with the most of pores between 1 and 10 μm. The

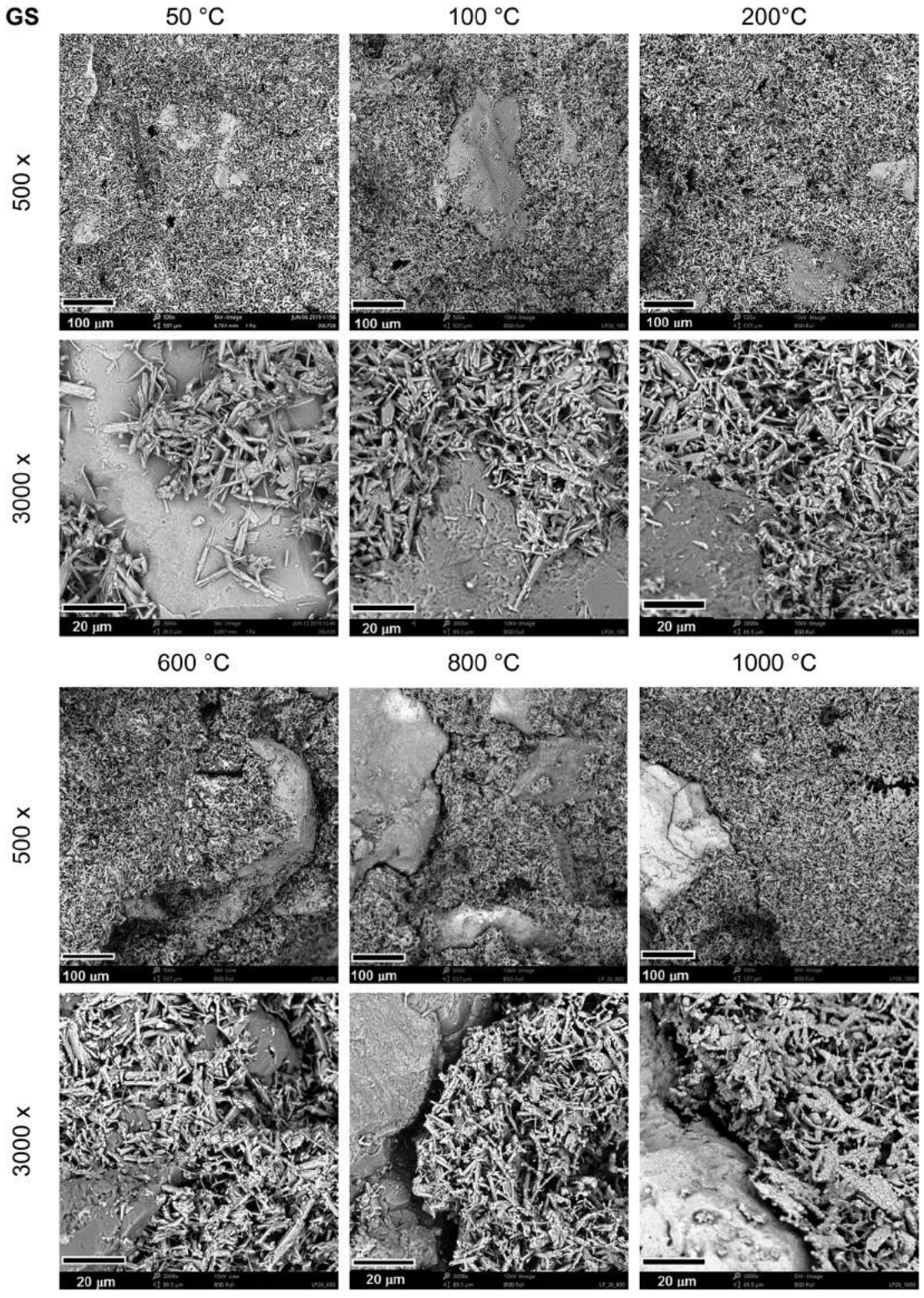


**Figure 7:** Microstructure of composite with silica sand at selected temperature.

composite with basalt contained also larger pores, which was caused by the higher amount of water in the material GB. It also had more very small pores under 0.01 µm, which is typical for materials with rougher aggregate particles; small pores were formed in the interfacial transition zone between the particles and gypsum matrix [17].

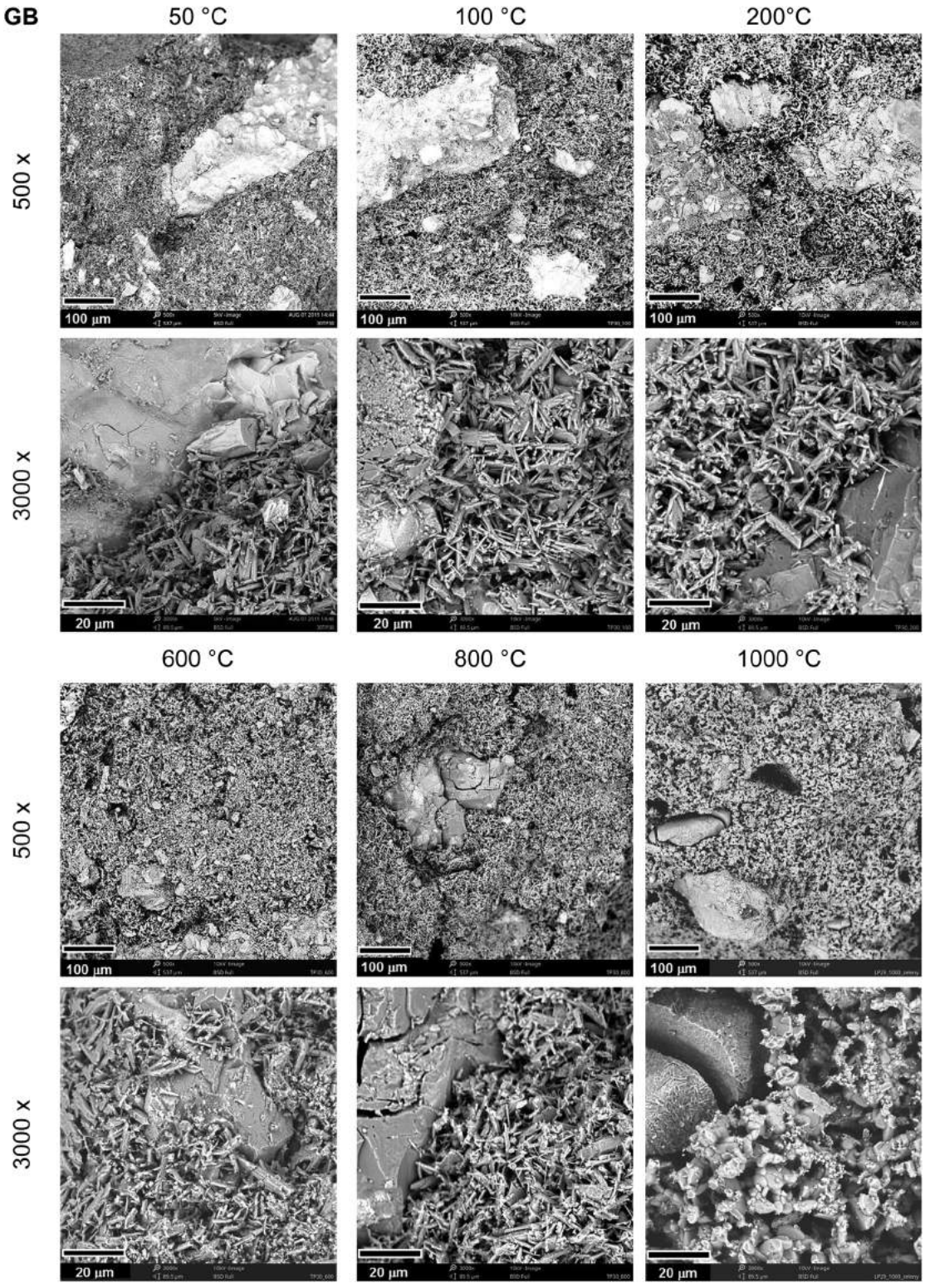


**Figure 8:** Microstructure of composite with basalt aggregate at selected temperatures.

The distribution curves of both composites did not change at 100°C; the total porosity continuously increased between 100 and 800°C, when it was highest in both materials. Mainly the finest pores increased from 100 to 600°C, while the amount of middle pores (1–10 µm) increased only slightly. The increase was caused by the released water

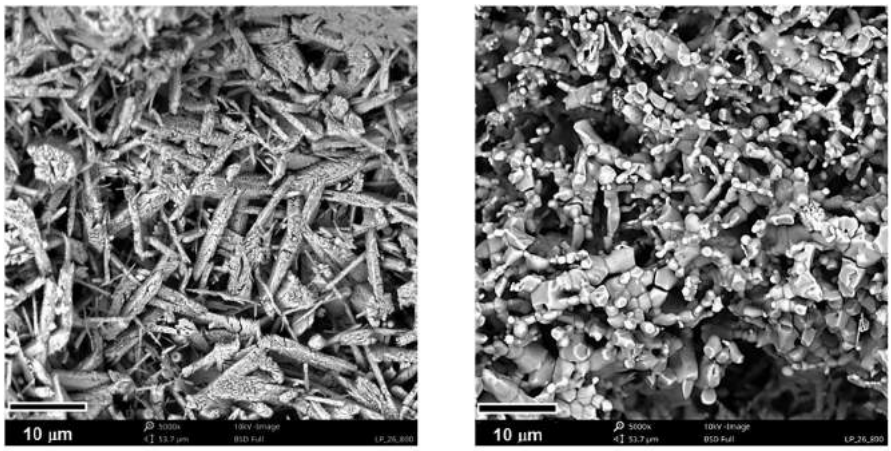


**Figure 9:** Crystal change at 800°C in composite with silica sand: (a) region with cracked crystals without shape change and (b) region with changed crystals.

during the dehydration of the gypsum. At 800°C also middle pores increased, because gypsum crystals started to change its size and shape, as was observed by SEM in some regions (Figure 9). The distribution curve changed substantially at 1,000°C. The finest pores disappeared and mostly pores with the size 10 µm or larger were formed in both materials. This change was related to the distinct change of the shape and size of gypsum crystals as observed by SEM.

## 5.4 Mechanical properties

Compressive strength of both composites is given in Figure 14. The original compressive strength of composite with basalt was slightly higher than compressive strength of composite with sand, even if it had higher porosity. This was given by the higher surface roughness of basalt particles. At 100°C the compressive strength of material with sand increased at 15%, which was probably caused

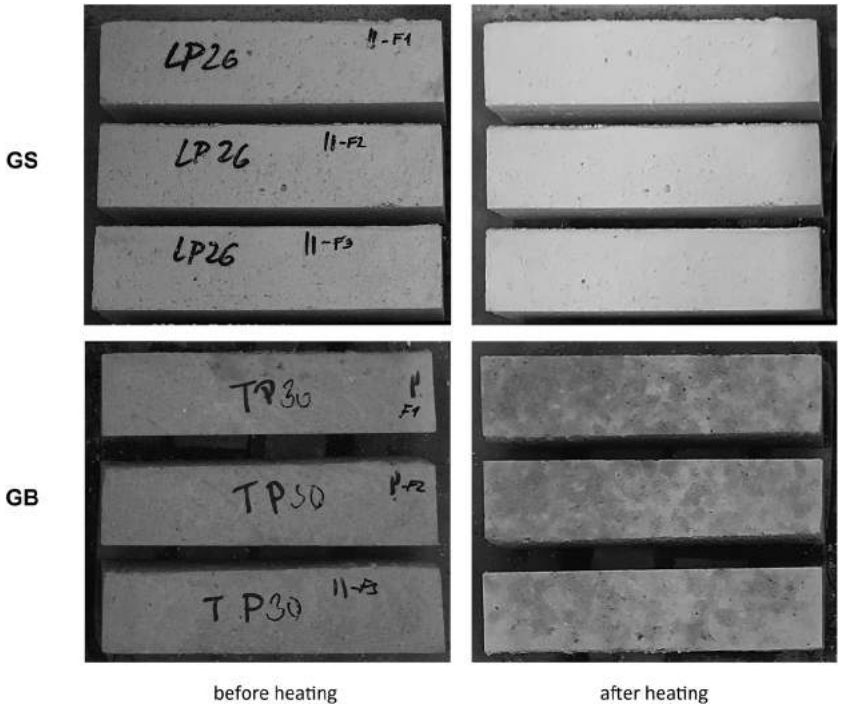


**Figure 10:** Samples of both composites before and after exposition to 1,000°C.

**Table 5:** Basic physical characteristic of composite with silica sand (GS)

| GS | | Temperature (°C) | | | | | | |
|---|---|---|---|---|---|---|---|---|
| | | 50 | 100 | 200 | 400 | 600 | 800 | 1,000 |
| Bulk density | (kg/m$^3$) | 1889.0 | 1891.0 | 1890.8 | 1818.0 | 1805.8 | 1764.3 | 1832.9 |
| Specific gravity | (kg/m$^3$) | 2754.2 | 2604.2 | 2704.7 | 2715.4 | 2727.7 | 2744.6 | 2732.6 |
| Total porosity | (%) | 31.4 | 27.4 | 30.1 | 33.1 | 33.8 | 35.7 | 32.9 |
| Volume change | (%) | 0 | 0.1 | 0 | −0.9 | −1.1 | −0.3 | −3.5 |

**Table 6:** Basic physical characteristic of composite with basalt (GB)

| GB | | Temperature (°C) | | | | | | |
|---|---|---|---|---|---|---|---|---|
| | | 50 | 100 | 200 | 400 | 600 | 800 | 1,000 |
| Bulk density | (kg/m$^3$) | 1919.0 | 1868.0 | 1801.3 | 1816.2 | 1837.6 | 1792.9 | 1872.4 |
| Specific gravity | (kg/m$^3$) | 2937.6 | 2812.8 | 2985.0 | 3036.2 | 3043.3 | 3054.6 | 3131.3 |
| Total porosity | (%) | 34.7 | 33.6 | 39.7 | 40.2 | 39.6 | 41.3 | 40.2 |
| Volume change | (%) | 0 | 0.3 | −0.4 | −1.2 | −1.9 | −4.3 | −6.8 |

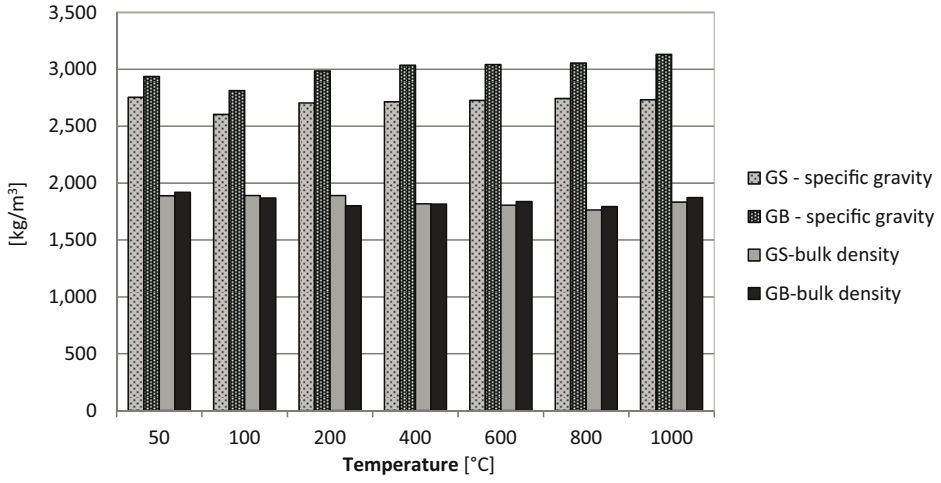


**Figure 11:** Specific gravity and bulk density after exposition to high temperatures.

by the hydration of residual bassanite. The strength of both materials decreased continuously at temperatures over 100°C with the exception of GS material at 800°C. Compressive strength of composite with sand increased from 3.4 MPa at 600°C to 4.1 MPa at 800°C. The increase was caused by the expansion of the silica sand which acted against the gypsum shrinkage. At the temperature 1,000°C, the compressive strengths of GS and GB were 1.2 and 1.3 MPa, respectively, which was 9.45 and 9.4% of original strength at 50°C.

The course of flexural changes is similar to the compressive strength changes (Figure 15). The flexural strength is less influenced by the surface roughness and more by the porosity; therefore, the flexural strength of composite with

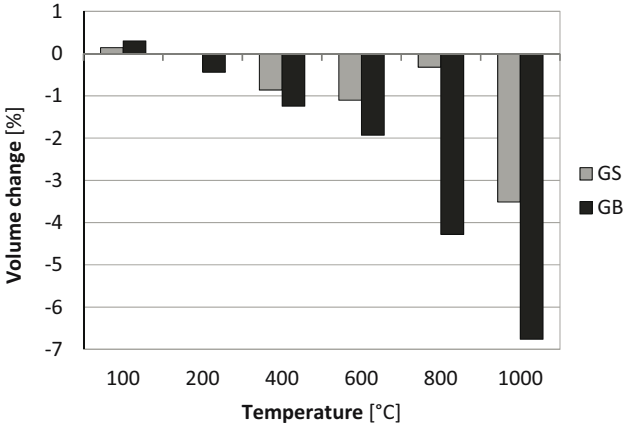


**Figure 12:** Volume changes of both composites after exposition to high temperatures.

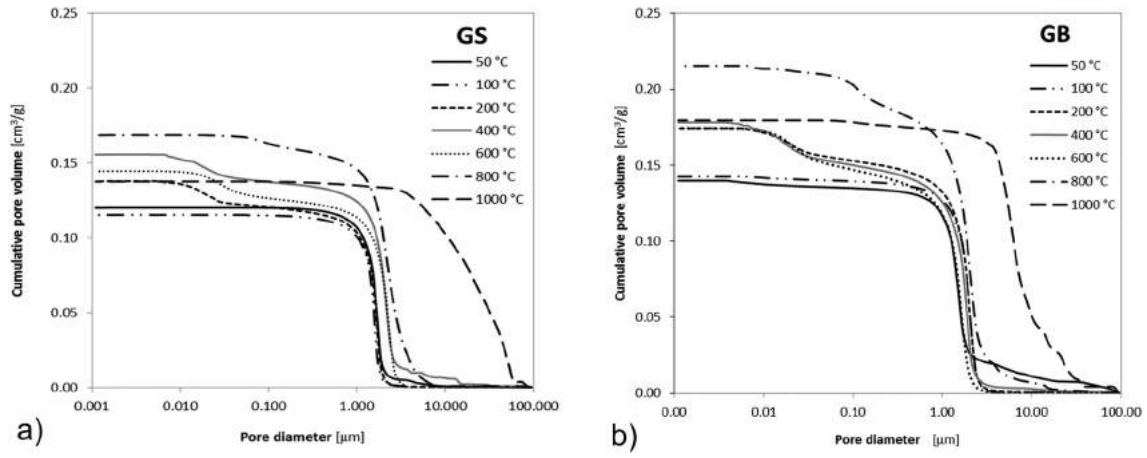


**Figure 13:** Pore size distribution curves after exposition to high temperatures: (a) GS and (b) GB.

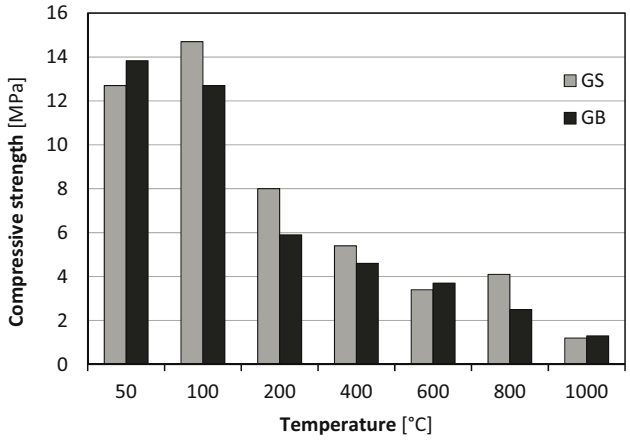


**Figure 14:** Compressive strength after exposition to high temperatures.

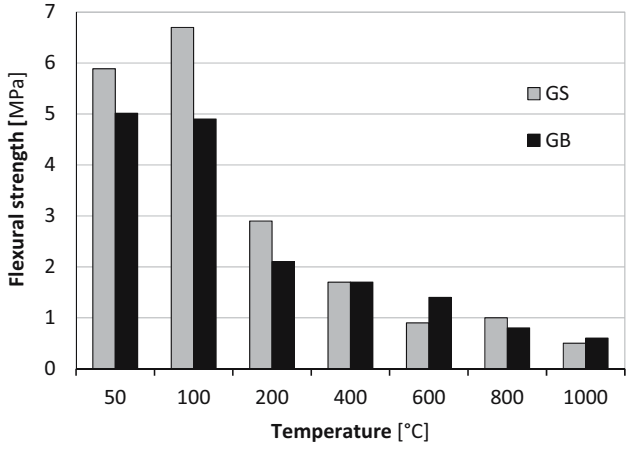


**Figure 15:** Flexural strength after heating.

basalt at 50°C was lower than the flexural strength of composite with sand, but the relative loss of strength of GB composite was lower. It was caused by the fact that the contact of aggregate particles and gypsum matrix was preserved while in the GS composite the contact zone was disrupted.

# 6 Conclusion

Behaviour and structure of gypsum composites with two types of solid nonporous aggregates at elevated temperatures were studied. Both materials maintained their integrity at all temperatures up to 1,000°C. The volume changes of composite with silica sand were smaller than volume changes of the composite with basalt aggregate. Nevertheless, even the volume change of composite with basalt aggregate was rather small, compared to the volume changes of pure gypsum paste, given in the literature. The residual compressive strength of both composites at 1,000°C was about 9.4% of original strength, which is better than the residual strength of cement-based materials, which are usually destroyed at this temperature [18] and comparable to geopolymers [19]. No spalling (contrary to concretes) was observed.

The microstructure of gypsum paste was changed similarly in both composites. The transition zone between the aggregate particles and gypsum matrix was disrupted in the composite with silica sand, while the transition zone in the composite with basalt stayed intact. It caused the higher loss of flexural strength in the composite with the silica sand.

There can be said that even if silica sand is not considered as a suitable aggregate in the cement concretes exposed to the high temperatures, it can be successfully

used in the gypsum-based materials, because its volume changes compensate the shrinkage of gypsum paste. The fire properties of the gypsum composite with silica sand were comparable or even better than fire properties of gypsum composite with basalt aggregate, which is usually considered as more suitable for the materials exposed to the elevated temperatures.

The future studies should be focused on the study of the gypsum-based materials with lightweight fillers at high temperatures. Inorganic lightweight fillers (perlite and vermiculite) are often used in commercial materials, and waste organic materials (foamed polystyrene and polyurethane) are studied very often because of environmental benefits, but their behaviour at high temperatures is not described yet sufficiently.

**Funding information:** This research was supported by the Czech Science Foundation, Project No. 19-08605S.

**Conflict of interest:** Authors state no conflict of interest.

## References

[1] Wirsching F. Calcium sulfate. Ullmann's encyclopedia of industrial chemistry. Weinheim, Germany: Wiley-VCH Verlag GmbH & Co; 2000. doi: 10.1002/14356007.a04_555.

[2] Karni J, Karni E. Gypsum in construction – origin and properties. Mater Struct. 1995;28:92–100. doi: 10.1007/bf02473176.

[3] Doleželová M, Scheinherrová L, Krejsová J, Vimmrová A. Effect of high temperatures on gypsum-based composites. Constr Build Mater. 2018;168:82–90. doi: 10.1016/j.conbuildmat.2018.02.101.

[4] Vimmrová A, Krejsová J, Scheinherrová L, Doleželová M, Keppert M. Changes in structure and composition of gypsum paste at elevated temperatures. J Therm Anal Calorim. 2020;142(1):19–28. doi: 10.1007/s10973-020-09528-8.

[5] Schroeder RA, Williamson RB. Post-fire analysis of construction materials – gypsum wallboard. Fire Mater. 2000;24(4):167–77.

[6] Fejean J, Lanos C, Melinge Y, Baux C. Behaviour of fire-proofing materials containing gypsum, modifications induced by incorporation of inert filler. Chem Eng Res Des. 2003;81:1230–6. doi: 10.1205/026387603770866434.

[7] Rozanski A, Rajczakowska M, Serwicki A. The influence of microstructure geometry on the scale effect in mechanical behaviour of heterogeneous materials. Sci Eng Compos Mater. 2017;24(4):557–71.

[8] Polyakova I. The main silica phases and some of their properties. In: Schmelzer J, editor. Glass. Berlin, Boston: De Gruyter; 2014. p. 197–268.

[9] Ringdalen E. Changes in quartz during heating and the possible effects on si production. JOM. 2015;67:484–92. doi: 10.1007/s11837-014-1149-y.

[10] EN 196-1. Methods of testing cement. Determination of strength. Brussels, Belgium: European Committee for Standardization; 2016.

[11] Földvári M. Handbook of thermogravimetric system of minerals and its use in geological practice. Budapest: Geological Institute of Hungary; 2011.

[12] Guggenheim S, Chang YH, Vangroos AFK. Muscovite dehydroxylation – high-temperature studies. Am Mineral. 1987;72:537–50.

[13] Doebelin N, Kleeberg R. Profex: a graphical user interface for the Rietveld refinement program BGMN. J Appl Crystallogr. 2015;48:1573–80. doi: 10.1107/s1600576715014685.

[14] EN 933-2. Tests for geometrical properties of aggregates. Determination of particle size distribution. Test sieves, nominal size of aperture. Brussels, Belgium: European Committee for Standardization; 1995.

[15] ČSN 72 1171. Determination of mass, porosity and voids ratio of aggregates. Czech Office for Standards (In Czech).

[16] EN 13454-2. Binders, composite binders and factory made mixtures or floor screeds based on calcium sulfate. Test methods. Brussels, Belgium: European Committee for Standardization; 2019.

[17] Scrivener KL, Nemati KM. The percolation of pore space in the cement paste aggregate interfacial zone of concrete. Cem Concr Res. 1996;26:35–40. doi: 10.1016/0008-8846(95)00185-9.

[18] Ma QM, Guo RX, Zhao ZM, Lin Z, He K. Mechanical properties of concrete at high temperature – a review. Constr Build Mater. 2015;93:371–83. doi: 10.1016/j.conbuildmat.2015.05.131.

[19] Aziz IH, Abdullah MMA, Yong HC, Ming LY, Hussin K, Surleva A, et al. Manufacturing parameters influencing fire resistance of geopolymers: a review. P I Mech Eng Part L J Mat. 2019;233:721–33. doi: 10.1177/1464420716668203.